LIQUID CRYSTAL NANO-PARTICLE COMPOSITES - DISPLAY APPLICATIONS

Abstract

In the past a large number of researches has been doned out to enhance the properties of LCs via different techniques, other than chemical synthesis. One technique to achieve this aim is the dispersion of NPs in liquid crystalline materials. Doping, i.e. the amalgamation of very small quantities of an additive into an LCs, is one of the important methods to enhance the properties of LCs. Liquid crystal–nanoparticles composites (LC-NPs) have emerged as a multidisciplinary field of research and attract great attention of scientists from the field of soft matter research as they can effectively be used to enhance the properties of LCs. Various types of nanomaterial are used to optimize the liquid crystal as per uses. The material of this chapter focuses on the enhancement of the electrical and electro-optical properties of nematic liquid crystals (NLCs) by mixing with nanoparticles. These LC-NPs composites are widely important for display applications.

Keywords: Liquid crystals, Nanoparticles, Liquid crystal naocomposites

Author

Mukesh Mishra
Faculty of Physical Sciences
Shri Ramswaroop Memorial University
Lucknow- Deva Road, Brabanki
Uttar Pradesh, India.

I. INTRODUCTION

A liquid crystal display (LCD) is a flat-panel display, electronic visual display, or video display that uses the light modulating properties of LCs. LCDs are convenient to display arbitrary images (as in general-purpose computer display) or fixed images which can be displayed or hidden, such as preset words, digits, and 7- segment displays as in a digital clocks. LCDs are used in large range of applications including computer monitors, televisions, instrument panels, aircraft cockpit displays, and signage. They are usual in consumer devices such as video players, gaming devices, clocks, watches, calculators, and telephones and have replaced cathode ray tube (CRT) displays in wide applications. Few researchers prepared a novel LCD device employing nematic materials instead of other liquid crystalline materials. NPs have shown an fascinating and feasible way of manipulating the properties of LCs, which will likely prove to be of significant importance for LC-based uses in devices and display applications. In this chapter nanocomposites have been prepared by dispersion of Barium titanate nanoparticles (BTNPs) in 4-pentyl-4'-cyanobipheny (5CB) nematic liquid crystalline material. Because of permanent dipole moment ferroelectric NPs (BTNPs) induce realignment of neighboring LC molecules, (i.e. parallel correlation between NPs and LCs) enhanced electro optical properties of LCs. To study the various display parameters in only N phase I have dispersed BTNPs in 5CB. 5CB is a basic display material and its thermodynamic [1-5], dielectric [6-20], and electro-optical [21-30] properties are reported earlier by several workers.5CB possesses only nematic (N) phase in the temperature range 17-34.5ºC [31-33]. The molecular structure of 5CB is shown in the Figure 5.1. BTNPs with a diameter of 100 nm have been procured from Sigma-Aldrich. Nanocomposites are prepared by dispersion of BTNPs in 5CB. In this chapter different dozes of (0.05, 0.5 and 5.0 wt % BTNPs) are dispersed and various physical parameters have been studied.

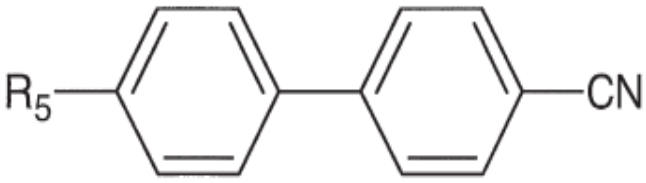

Figure 1: .Molecular structure of 4-pentyl-4'-cyanobiphenyl (5CB) [7].

II. RESULTS AND DISCUSSION

1. **Thermodynamic Study:** Amalgamation of BTNPs in NLC was studied under PLM. This method explains the first result if a particular nanomaterial signs to aggregates [34]. There is no any proof of aggregation of NPs during analyzing the nanocomposites in the N phase under PLM. DSC was used to find the effect of BTNPs on the nematic-isotropic transition temperature (T_{NI}) or isotopic-nematic transition temperature (T_{IN}) in the heating and cooling phases. Precise observations of transition temperatures of liquid crystal-nanoparticles composites (LC-NPs) are required to examine the fruitfulness for liquid crystal display (LCD) applications [35]. Nanocomposite materials have been provided 5

thermal cycles before writting original data in order to sustain the system. DSC thermograms of pure 5CB and its nanocompositesare shown in heating and cooling cycles **(Figure 1.2a & b)** at the scan rates of 5.0 °C min^{-1}. A heating and cooling rate dependent observations of all transitions of 5CB and its nanocomposites has been performed. DSC was drive at different scanning rates between 2.5 °C min^{-1} and 15 °C min^{-1}. As the scan rate decreases, all transitions move toward lower temperature in the case of heating whereas shift toward higher temperature in the cooling [36].

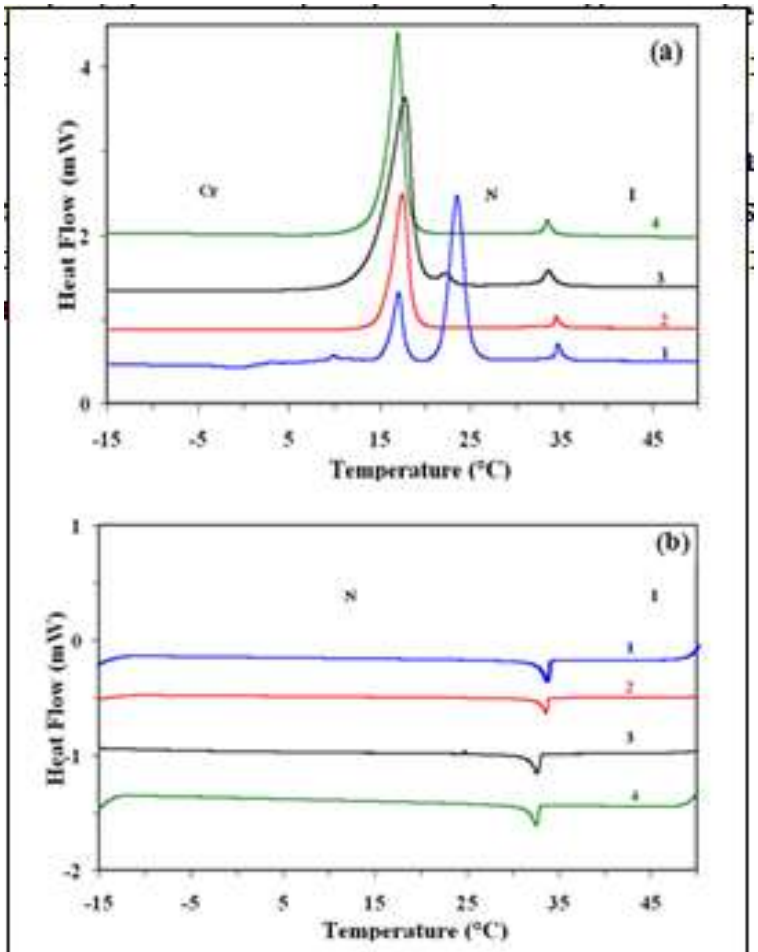

Figure 1.2: DSC thermograms for the (a) heating and (b) cooling cycles of pure 5CB and its nanocomposites . Curves 1, 2, 3 and 4 are for pure 5CB, 5CB + 0.05 wt % BTNPs, 5CB + 0.5 wt % BTNPs and 5CB + 5.0 wt % BTNPs, respectively.

Extrapolated transition temperatures at the scan rate of 0 $^{\circ}$C min^{-1} have been found through least square fit [37] which give following phase sequences in the heating and cooling cycles:

- Heating cycles:

  5CB: Cr-(17.0 $^{\circ}$C)-N-(34.5 $^{\circ}$C)-I
  5CB + 0.05 wt% BT NPs: Cr-(16.9 $^{\circ}$C)-N-(34.2 $^{\circ}$C)-I
  5CB + 0.5 wt% BT NPs: Cr-(16.6 $^{\circ}$C)-N-(33.2 $^{\circ}$C)-I
  5CB + 5.0 wt% BT NPs: Cr-(16.5 $^{\circ}$C)-N-(33.1 $^{\circ}$C)-I

- Cooling cycles:

  5CB: I-(34.0 $^{\circ}$C)-N
  5CB + 0.05 wt% BT NPs: I-(33.8 $^{\circ}$C)-N
  5CB + 0.5 wt% BT NPs: I-(32.9 $^{\circ}$C)-N
  5CB + 5.0 wt% BT NPs: I-(32.8 $^{\circ}$C)-N

Pure 5CB have been studied by different researchers [1-5]. From the experimental observations, it is noted that the transition temperatures, i.e. T_{NI} (or T_{IN}) of the nanocomposite are sifted downwards as to pure 5 CB. Neither of the pure 5CB and its nanocomposite samples crystallizes up to lowest temperature i.e. up to -15 °C. From the above-mentioned DSC data we are concluded that enhancing the concentartion of BTNPs, decreases the T_{NI} (also T_{IN}), which also proven by PLM. Most important experiments showed that the mixing of the ferroelectric NPs (BTNPsand $Sn_2P_2S_6$) leads to an increase in the T_{NI} of the nanocomposites [38-41], but a decrease of T_{NI} in few experiments was also shown [42-45]. In this experiment there is an significant decrease in the T_{NI} as the concentration of BTNPs in 5CB increases. In the case of 5CB + 0.05 wt% BTNPs, T_{NI} decreases by ~0.3 °C, in 5CB + 0.5 wt% BTNPs, it decreases by 1.3 °C, while in 5CB +5.0 wt% BTNPs, it decreases by 1.4 °C. According to Gorkunov and Osipov [46] due to the spherical NPs, the average distance between mesogenic molecules of the liquid crystal (LC) matrix is enhanced and then LC matrix is diluted. This decreases the strength of intermolecular interactions, decreases the Nematic ordering and decreases the transition temperature in to the N phase. Lopatina *et al*. [47] have shown that the dipolar induction interaction between ferroelectric NPs and the surrounding NLC medium may result in a substantial decrease of the $T_{IN.}$ According to Gupta *et al.* [48] another cause of reducing in T_{NI} (or T_{IN}) is that BTNPs increase the disorder in the system and destabilize the liquid crystalline phase. From the thermodynamic data, it is concluded that at low concentrations (<1wt %), T_{IN} reduces rapidly with increasing concentration. But at higher concentrations (>1wt %), T_{IN} decreases with slow pace as compared to low concentrations. Same results are also reported by Gorkunov*et al* [49]. at low NP concentrations, there is no chance of phase separation and decrease in the T_{IN} is due to dilution effect, whereas at higher concentration phase separation may take place within a range of NPs concentrations. Vardanyan *et al* have been reported that only a fraction of NPs are homogeneously mixed in LC matrix but higher concentration shows aggregation of NPs [50]. These studies also suggest that for low concentrations, due to the good miscibility, T_{IN} decreases rapidly with the increasing concentration whereas while going

in high concentration region, decrease of T_{IN} gets slow. The Latter seems due to the development of phase separation.

2. **UV-Vis Study:** The spectra for 5CB, BTNPs and its nono dispersed sample are shown in **Figure 1.3.** The 5CB plot gives a longest absorbance at wavelength (λ_{max}) of 302 nm and BTNPs show λ_{max} at 285 nm **(see inset of Figure 1.3).** These findings are in good with respective λ_{max} reported in literatures [51, 52]. The optical band gap of pure 5CB, BTNPs and its nano composites have been calculated using relation [53, 54]

$$\alpha\nu = B(\nu - E_g)^m \qquad \textbf{(1.1)}$$

Where α is the absorption coefficient ($\alpha = \frac{2.303\times A}{l}$, where l and A are the path length of the cell and absorbance), ν is the photon energy, E_g is the optical band gap. Exponent m is an index which assumes the values 1/2, 2, 3/2 and 3 corresponding to the direct allowed, indirect allowed, forbidden direct and forbidden indirect transitions, respectively.

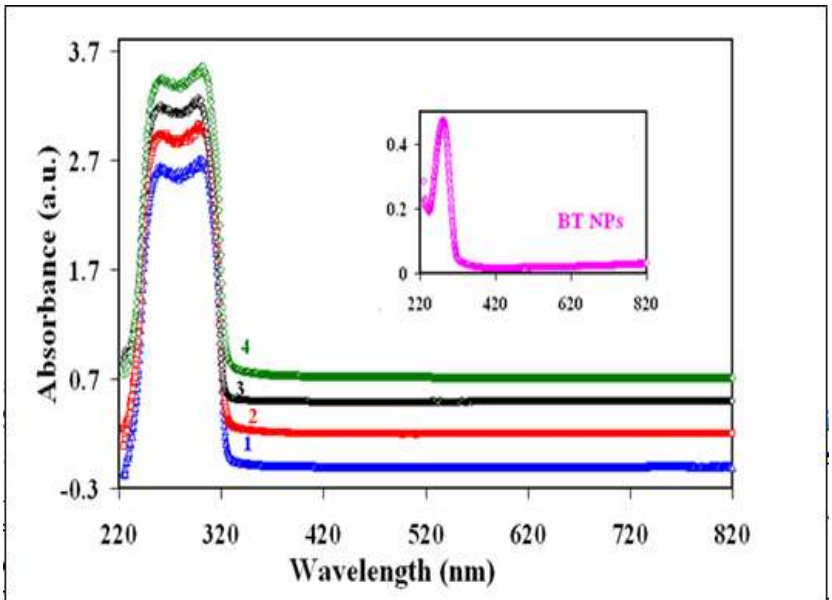

Figure 1.3:UV-Vis absorption spectra for the pure 5CB and its nanocomposites. Curves 1, 2, 3 and 4 are for pure 5CB, 5CB + 0.05 wt % BTNPs, 5CB + 0.5 wt % BTNPs and 5CB + 5.0 wt % BTNPs, respectively. Inset (a) shows absorbance of BTNPS.

The best correlation is obtained by scheming $(\alpha h\nu)^2$ vs. ν, demonstrating that the E_g of pure 5CB and its nanocomposites is due to the direct allowed transitions (for m= ½ the fitting parameters chi^2=0.00012 and R^2=0.99587)[55-57]. Thus the values of E_g have been deliberate by plotting $(\alpha\nu)^2$ versus ν and extrapolating the linear portion of the plot to $(\alpha h\nu)^2$=0 **(see Equation1.1)**. E_g plots for pure BTNPs is shown in **Figure1.4**. The calculated E_g of BTNPs from the intercept of the straight line at α = 0 has been found to be 4.03 eV. According to Wemple*et al.* [58] particles larger than 15 nm, E_g is about equivalent to that of barium titanate in bulk. E_gPlots for pure 5 CB, and its nanocomposites are shown in **Figure 1.5**. The E_g of pure 5CB has been found to be 3.82

eV **(seeFigure1.5a)**. E_g for5CB + 0.05 wt% BTNPs (**Figure 1.5 b)**, 5CB + 0.5 wt% BT NPs (**Figure 1.5 c)** and 5CB +5.0 wt% BTNPs (**Figure 1.5 d)** have been determined to be 3.80 eV, 3.82 eV and 3.81 eV respectively. Diminution in E_g for 0.05 wt% BTNPs is accountable for the boost in the conductivity.

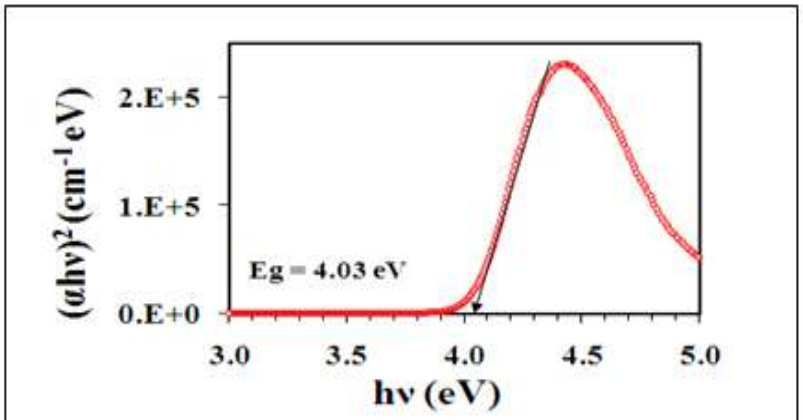

Figure 4: Determination of optical band gap (E_g) of pure BTNPs.

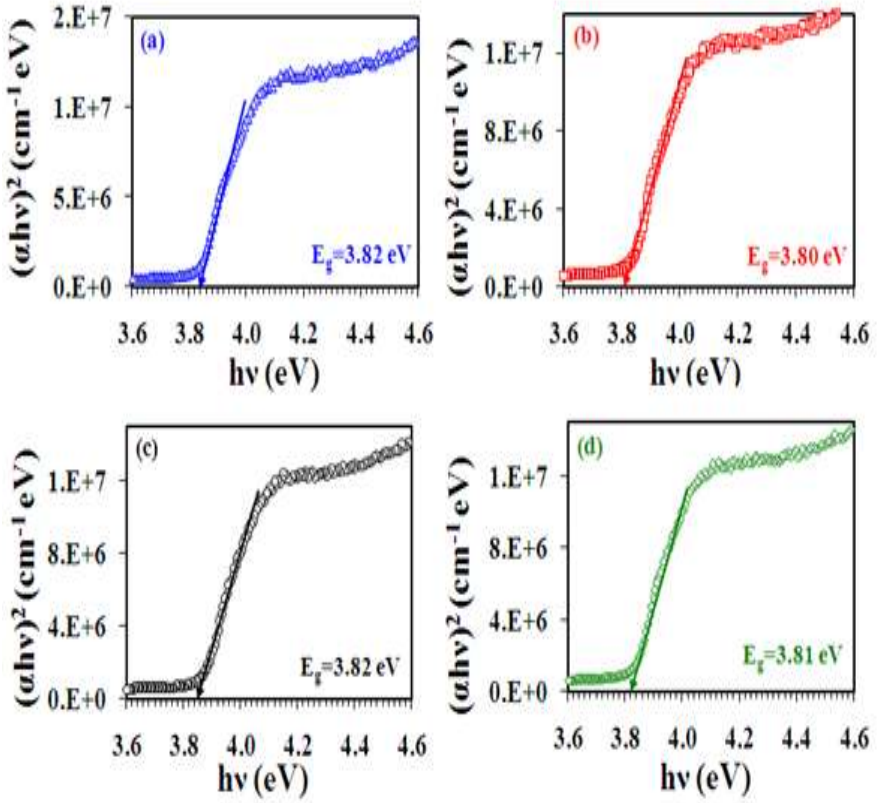

Figure 5: Determination of the optical band gap (E_g) of pure 5CB and its nanocomposites. Figure a, b, c and d are for pure 5 CB, 5CB + 0.05 wt % BTNPs, 5CB + 0.5 wt % BTNPs and 5CB + 5.0 wt % BT NPs, respectively.

3. **Electro-Optical Study:** In **Figure 1.6** transmission intensity with voltage is plotted for pure 5CB and its nanocomposites in nematic phase at 23 °C, which provide knowledge regarding threshold (V_{th}), switching voltage (ΔV) and the steepness (slope) of the transmission voltage curve (TVC). Bright and dark states are found under the PLM at the lower and higher applied voltage respectively due to the reorientation of nematic molecules along the direction of external applied voltage. The reorientation of nematic directors with the reason of electric field from bright state **(Figure 1.6 Inset a)** to dark state **(Figure 1.6 Inset b)** is also known as Freedericksz transition [59, 60]. The voltage necessary to attain transition is called threshold voltage (V_{th}). At small voltages less than V_{th} molecule lie in the planar alignment and therefore a bright condition is observed. When the applied voltage is increased above V_{th} the molecules step by step turn to the homeotropic orientation and a dark state is observed.

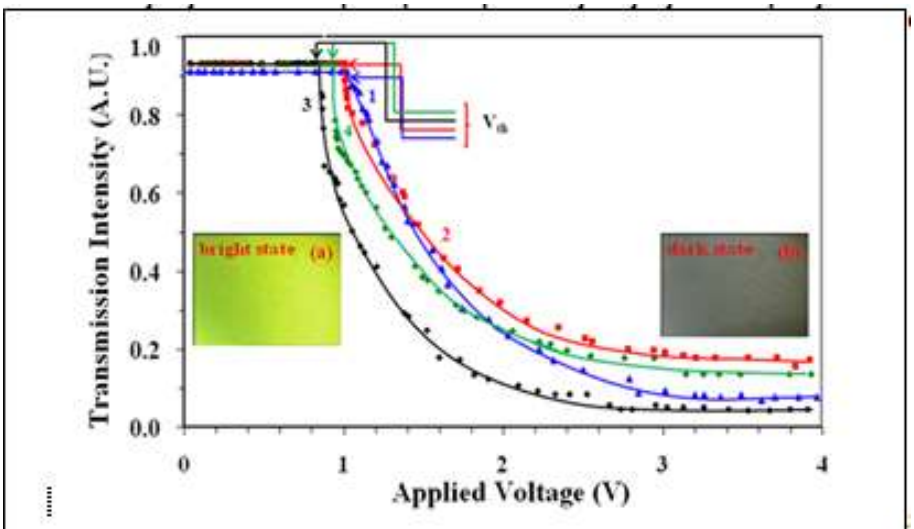

Figure 6: Transmission voltage (T-V) curves for pure 5CB and its nanocomposites to the applied voltage of frequency 1 kHz. Curves 1, 2, 3 and 4 correspond to the pure 5CB, 5CB + 0.05 wt % BTNPs, 5CB + 0.5 wt % BTNPs and 5CB + 5.0 wt % BTNPs, respectively. Insets (a and b) show bright and dark state of the cell filled with 0.5 wt% of BTNPs dispersed in 5CB respectively.

The ΔV is taken as$V_{90} - V_{10}$, where $V_{90}$and $V_{10}$are the voltages resultant to the transmission intensity of 90% and 10% of the maximum value. The lower value of ΔV (~0.5-1.0) is helpful for the applications. High steepness of the slope ($=(I_{90} - I_{10})/V_{90} - V_{10}$)) of the TVC is also useful. I have illustrated the character of dielectric anisotropy($\Delta\varepsilon'$), in order to view the electro-optic parameters, where $\Delta\varepsilon' = \varepsilon'_{\|} - \varepsilon'_{\perp}$, $\varepsilon'_{\|}$ and $\varepsilon'_{\perp}$ are the longitudinal and transverse components of relative permittivity respectively. The variations of $\varepsilon'_{\|}$ and $\varepsilon'_{\perp}$ components of relative permittivity of the host 5CB along with its nanocomposites on temperature scale are shown in **Figure 1.7**. The values of the $\varepsilon'_{\|}$ and $\varepsilon'_{\perp}$for pure 5CB are in good with the literature data [61].

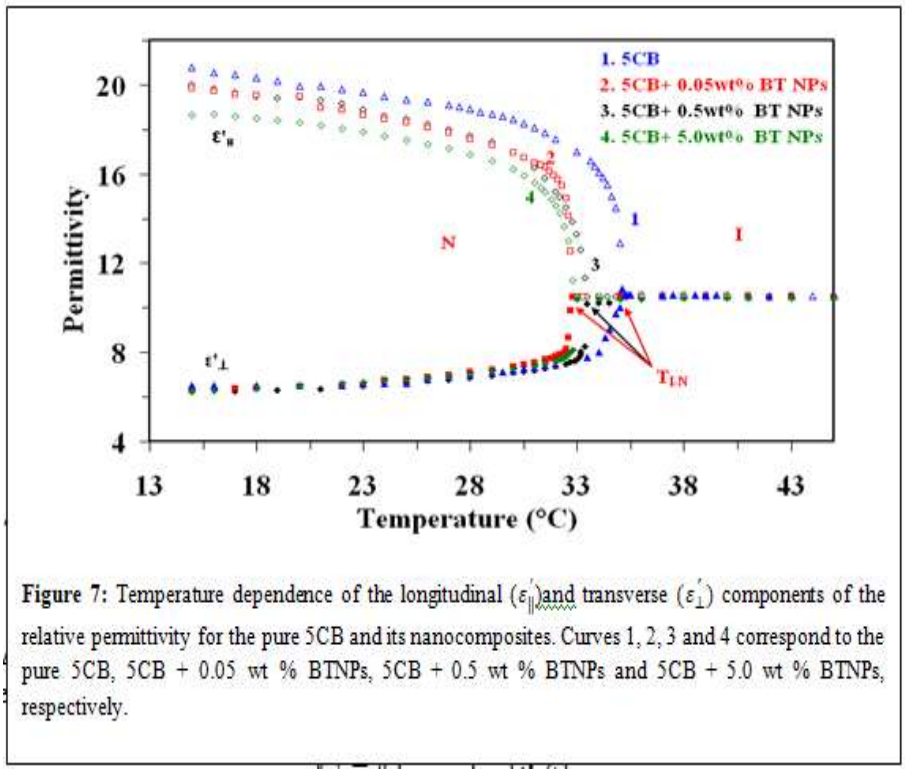

Figure 7: Temperature dependence of the longitudinal ($\varepsilon_{\parallel}^{'}$)and transverse ($\varepsilon_{\perp}^{'}$) components of the relative permittivity for the pure 5CB and its nanocomposites. Curves 1, 2, 3 and 4 correspond to the pure 5CB, 5CB + 0.05 wt % BTNPs, 5CB + 0.5 wt % BTNPs and 5CB + 5.0 wt % BTNPs, respectively.

Figure 1.7 shows that the $\varepsilon_{\perp}^{'}$ is approximately unaffected with the escalating concentration of BTNPs, while the $\varepsilon_{\parallel}^{'}$component significantly decreases in dissimilarity to the outcome reported previously [40, 61]. Therefore $\Delta\varepsilon^{'}$decreases with the increasing concentration of BTNPs. $\Delta\varepsilon^{'}$participated an imperative character in the process of twisted NLCs displays. The $V_{t\square}$is given by [60, 62-64]

$$V_{t\square} = \pi\left(\frac{K_{11}}{\varepsilon_0 \Delta\varepsilon^{'}}\right)^{1/2} \quad (\mathbf{5.2})$$

Where k_{11} is the splay elastic constant of the material and has been predictable by using the experimental values of $V_{t\square}$ and $\Delta\varepsilon^{'}$. From the equation, it can be seen that $V_{t\square}$ is directly proportional to the square root of k_{11} and inversely proportional to the square root of $\Delta\varepsilon^{'}$of the material. $k_{11}$is also directly proportional to square of order parameter (S^2) and $\Delta\varepsilon^{'} \propto S$; then we have $V_{t\square} \propto \sqrt{S}$ [65]. $\varepsilon_{\parallel}^{'}$,$\varepsilon_{\perp}^{'}$and average ($\varepsilon^{'}$= ($\varepsilon_{\parallel}^{'}$+ 2 $\varepsilon_{\perp}^{'}$)/3) components of the permittivity, $\Delta\varepsilon^{'}$, ratio of the $\Delta\varepsilon^{'}/\varepsilon_{\perp}^{'}$, $V_{t\square}$,ΔV, slope of the TVC ($= (\Delta I/\Delta V) = (I_{90} - I_{10}/(V_{90} - V_{10}))$, and k_{11} are given in **Table 1.1** for the N phase at 23.0 °C. $V_{t\square}$ may decrease as the order parameter decreases (i.e. $\Delta\varepsilon^{'}$) due to the existence of suitable NPs. Note that the decrease in the $V_{t\square}$ observed in previous studies [61] was accounted by assuming that k_{11} remains unaffected with the accumulation of the NPs, while experimentally an increase in $\Delta\varepsilon^{'}$ was observed. However in current exploration, I find that both k_{11} and $\Delta\varepsilon^{'}$ decreases with adding of NPs. Such drop of the Freedericksz$V_{t\square}$and of the S induced by inorganic magnesium oxide (MgO) NPs in the N phase has also been reported earlier [66]. In this study primarily for 0.05 wt% of BTNPs mixed sample, the decrease in the $\Delta\varepsilon^{'}$ is 5% and the ulter in the value of K_{11} is 32% **(see Table 1.1)** which is eventually decreasing the $V_{t\square}$by only ~2% as compared to that of

pure sample. However for 0.5 wt% of BTNPs composites, decrease in the $\Delta\varepsilon'$ is 7% and the change in the value of K_{11} is 52%, hence decreasing the $V_{t\square}$ by about 17% compared to pure sample. On the other hand $V_{t\square}$ for higher concentration (>1 wt %) is not distorted as much predicted. $V_{t\square}$ for 5.0 wt% of BTNPs has decreased by 8%, at the same time K_{11} and $\Delta\varepsilon'$ decreases by 46% and 14 % respectively. Reznikov *et al.* [61] has reported that higher concentration (>2-3 wt %) of submicron particles create almost rigid liquid crystal suspension. Due to this, $V_{t\square}$ does not change significantly for 5.0 wt% of BTNPs dispersed systems. From **Table 1.1**, we can infer that ΔV decreases as concentration of BTNPs increases i.e. up to 0.5 wt %, at the same time steepness of the T-V curve increases. Decrease in the ΔV is mostly accountable for the enhancement in the steepness of T-V curve. For 0.5 wt% of BTNPs, ΔV and steepness are unaffected compared to the pure sample.

Table 1: Longitudinal $(\varepsilon'_{\parallel})$, transverse $(\varepsilon'_{\perp})$ and average $(\varepsilon' = (\varepsilon'_{\parallel} + 2\,\varepsilon'_{\perp})/3)$ components of the relative permittivity, dielectric anisotropy $(\Delta\varepsilon')$, ratio of dielectric anisotropy to the transverse component of the relative dielectric permittivity $(\Delta\varepsilon'/\varepsilon'_{\perp})$, threshold voltage ($V_{th}$ in Volts), switching voltage (ΔV in volts), ratio of $\Delta I/\Delta V$ (in V^{-1}) and splay elastic constant (K_{11} in pN) in the N (at 23.0 °C) phase.

concentration	$\varepsilon'_{\parallel}$	$\varepsilon'_{\perp}$	$\varepsilon' = (\varepsilon'_{\parallel} + 2\,\varepsilon'_{\perp})/3$	$\Delta\varepsilon'$	$\Delta\varepsilon'/\varepsilon'_{\perp}$	V_{th}	ΔV	$\Delta I/\Delta V$	K_{11}
5 CB	19.6	6.5	10.8	13.1	2.0	1.02	1.25	0.64	16.50
0.05wt% BT NPs	18.9	6.5	10.6	12.4	1.9	1.00	1.06	0.75	11.13
0.5wt% BT NPs	18.7	6.5	10.5	12.2	1.9	0.85	0.99	0.80	7.91
5.0wt% BT NPs	17.9	6.7	10.4	11.2	1.7	0.94	1.20	0.66	8.88

4. **Dielectric Study:** Dielectric anisotropy of the N phase is governed by the Maier and Meier theory [67]

$$\Delta\varepsilon' = \frac{NHF}{\varepsilon_O}\left[\Delta\alpha - \frac{F}{2kT}P^2(1 - 3cos^2\beta)\right]S \quad (\mathbf{5.3})$$

Where M is the number density of molecules and S is the order parameter, $\Delta\alpha$ is the anisotropy of the polarisability, P is the resultant dipole moment of the molecule, β is the angle between the dipole moment and the long axis of the molecule and F is the feedback factor and $H = 3\varepsilon'(0)/(2\varepsilon'(0) + 1)$. According to **Equation (1.3)**, $\Delta\varepsilon'$ appreciably depends upon both N and S. N is predictable to decrease with the amplify in the doping concentration of BTNPs and due to the $\Delta\varepsilon'$ decreases with the increasing concentration of BTNPs. one more cause is that order parameters of LC and ferroelectric NPs interrelate with each other and the dipole moments of ferroelectric NPs join anti-parallell to dipole moments of NLC molecules. This corresponds to a lesser value of $\varepsilon'_{\parallel}$ and hence $\Delta\varepsilon'$ according to the Kirkwood *et al.* [68]. According to Vardanyan et al.

[69], NPs increase the relative number of 5CB dimmers, which in turn decrease the $\Delta\varepsilon'$ of the system.

Frequency dependence of $\varepsilon_{\perp}'$ for the pure 5CB and its nanocomposites shows that data are approximately invariant up to 10MHz. This indicates that there is no relaxation mechanism for the planar orientation of molecules in the frequency window of our measurements. Therefore, I could not find out the relaxation frequency corresponding to the molecular rotation about the long axis. However, it could be feasible to observe a relaxation mechanism in the homeotropic aligned molecules due to the rotation of about their short axes [70-72].

The variations of the experimental data of $\varepsilon_{\|}'$and $\boldsymbol{\varepsilon}_{\|}''$with frequency in the N phase are shown in **Figure 1.8** for pure 5CB and its nanocomposites. The data of permittivity ($\varepsilon_{\|}'$) and loss ($\square_{\|}$) for 5CB and its nanocomposites lie on the Cole-Cole semi circles as shown in **Figure 1.9.**From the value of the distribution parameter obtained from the fitting of the experimental data as well as from the Cole-Cole [73-75] plots shown in **Figure1.9** (plots are complete semi circles), it is evident that the observed relaxations are a typical Debye process [76, 77].

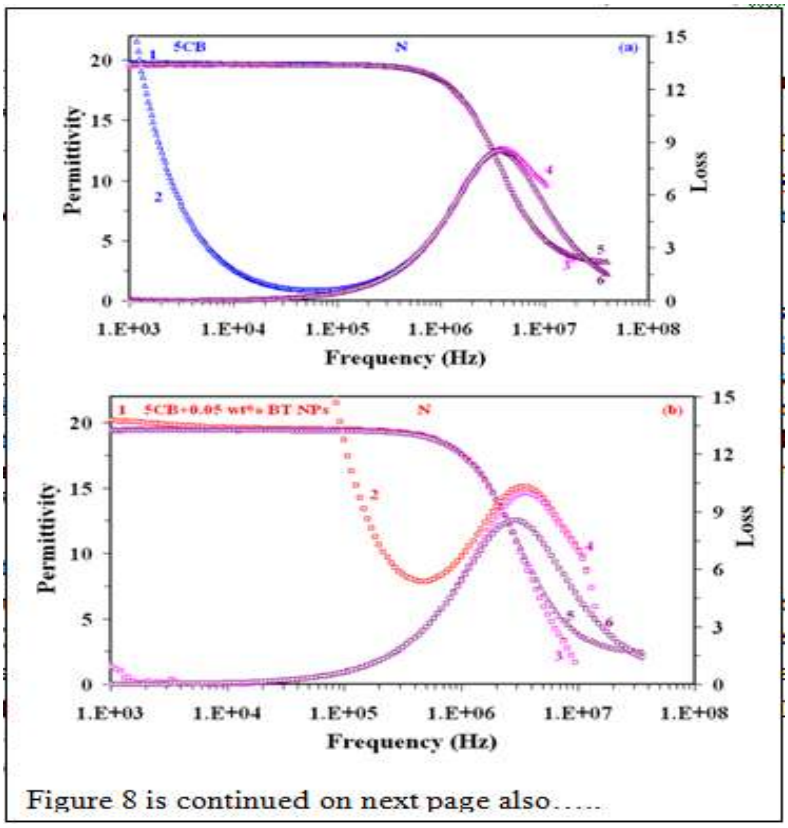

Figure 8 is continued on next page also.....

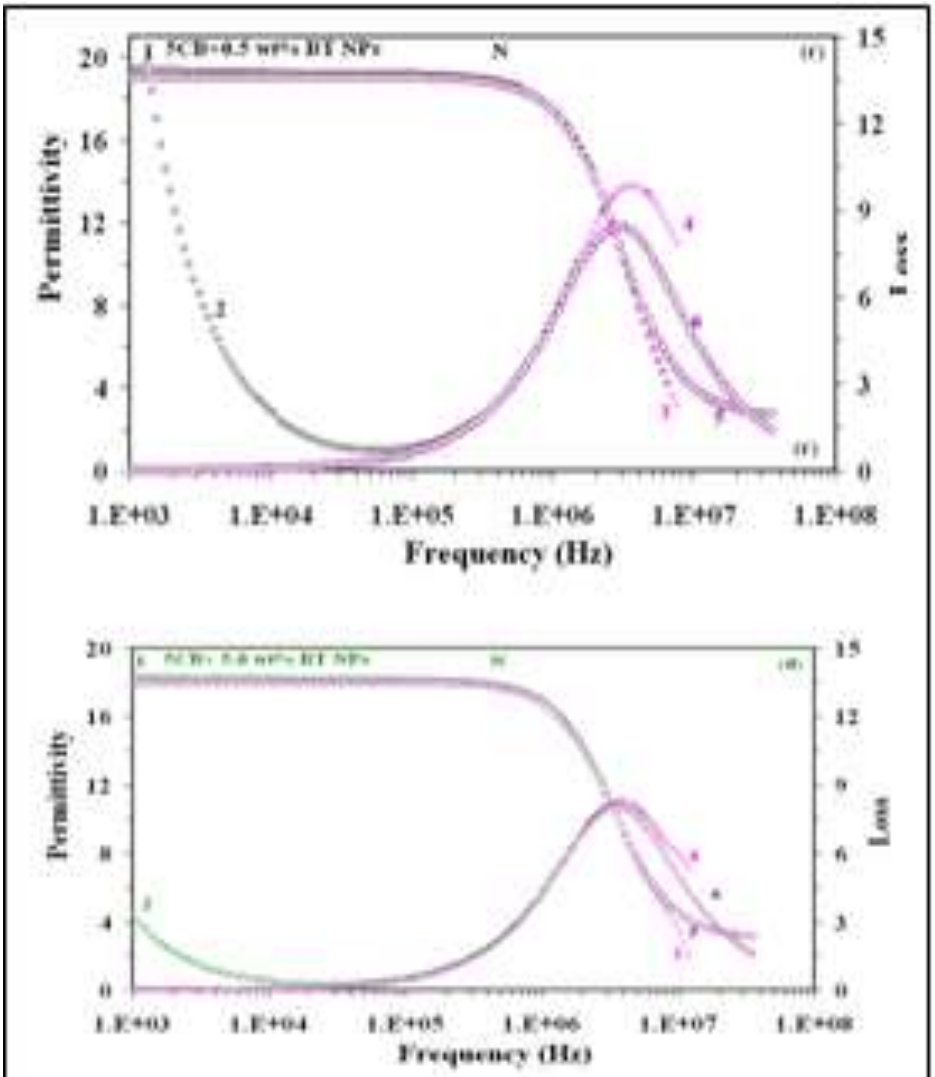

Figure 8: Frequency dependence of the longitudinal component of the relative permittivity ($\varepsilon_{\parallel}'$) and the loss ($\varepsilon_{\parallel}''$) in the N phase (23.0 °C). Curves 1 and 2 show the measured value of $\varepsilon_{\parallel}'$ and $\varepsilon_{\parallel}''$. Curves 3 and 4 represents the corrected data for $\varepsilon_{\parallel}'$ and $\varepsilon_{\parallel}''$ obtained by subtracting the high and low frequency corrections from the measured data. Curves 5 and 6 are the generated data of $\varepsilon_{\parallel}'$ and $\varepsilon_{\parallel}''$ after low and high frequency corrections. Figure(a) 5CB, (b) 5CB + 0.05 wt % BTNPs, (c) 5CB + 0.5 wt % BTNPs and (d) 5CB + 5.0 wt % BTNPs dispersed samples.

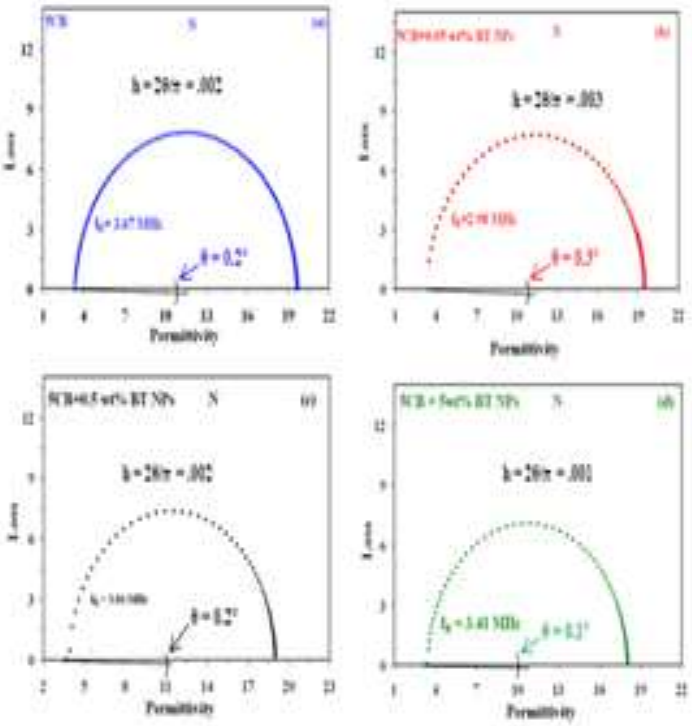

Figure 9: Cole-Cole plots showing the variation of loss (ε_i') with permittivity (ε_i')for the pure 5CB and its nanocomposites in the nematicphase (23.0 °C). Figure(a) Pure 5CB, (b) 5CB + 0.05 wt % BTNPs, (c) 5CB + 0.5 wt % BTNPs and (d) 5CB + 5.0 wt % BTNPs dispersed samples.

The variation of relaxation frequency 〖(f〗_R) with the inverse of the temperature is shown in Figure 1.10.f_Rof the pure 5CB is 3.54 MHz in the N phase (at 23.0 °C) (see Figure 1.8 (a)). The experimental values of the f_R are in good conformity with the data [78] reported previously. The observed values of f_Rat 23 °C for 0.05 wt% BTNPs, 0.5 wt% BTNPs and 5.0 wt% BTNPs dispersed in 5CB are 2.98 MHz, 3.0 MHz and 3.37 MHz respectively. These data recommend that f_R corresponding to flip flop motion of the molecules about the short axis is slightly decreased in the case of nanocomposites as compared to pure 5CB.

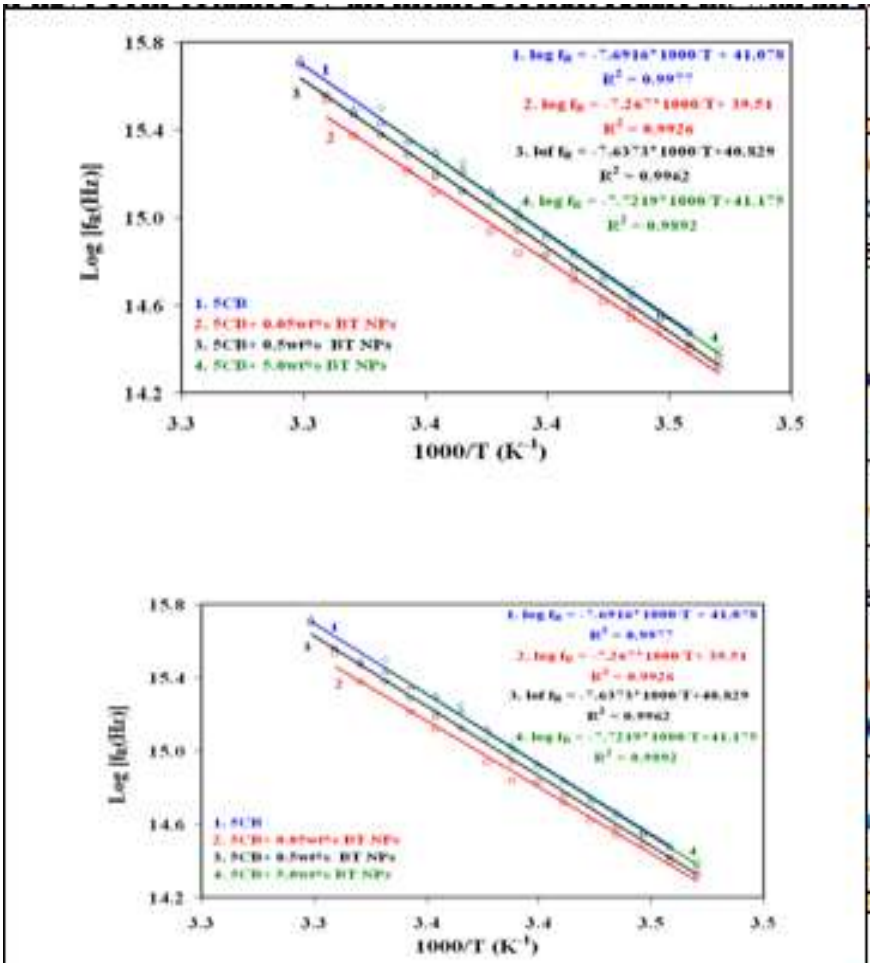

Figure 10: Variation of relaxation frequency (f_R) with inverse of absolute temperature (K^{-1}) showing Arrhenius behaviour of the observed relaxation mode. Curves 1, 2, 3 and 4 correspond to the pure 5CB, 5CB + 0.05 wt % BTNPs, 5CB + 0.5 wt % BTNPs and 5CB + 5.0 wt % BTNPs respectively.

The activation energy(W_A)for the observed relaxation process was determined by the Arrhenius equation [79, 80]

$$\log f_R = \log f_0 - W_A / N_A\ kT \qquad (1.4)$$

Where, W_Ais the activation energy, N_A is the Avogadro number, k is the Boltzmann constant and T is the absolute temperature. From Figure 1.10, slopes of log f_Rvs inverse of temperature plots have been obtained by the method of least square fit. With the help of slopes of the straight lines, W_A have been obtained for 5 CB and its nanocomposites.I have determinedW_Aof 63.9 kJ mol-1 for the pure 5 CB sample in the N phase. The observed values of the W_A are in good agreement with the data [78] reported earlier. The observed W_Aare 60.3 kJ mol-1, 63.5 kJ mol-1, 64.2 kJ mol-1 for 0.05 wt% BTNPs, 0.5 wt% BTNPs and 5.0 wt% BTNPs dispersed in 5CB respectively.

From above mentioned results, it is concluded that⟦ W⟧_Ahas decreased for 0.05 wt% BTNPs. However, for other concentrations, ⟦ W⟧_A increases.

The frequency dependence of the total conductivity parallel ($\sigma_{\parallel}$) to the director of 5CB and its nanocomposites are shown in **Figure 1.11 (a)** in N phase at 23.0 °C. From figure it is observed that at low frequencies conductivity is constant while at higher frequencies it frequency dependent [81, 82]. Temperature dependence of longitudinal ionic conductivity ($log\sigma_{i\parallel}$) is shown in **Figure 1.11 (b)**. It can be seen that for 0.05 wt% BTNPs composite system, $\sigma_{i\parallel}$ increases by two orders of magnitude and for 0.5 wt% BTNPs composites $\sigma_{i\parallel}$ is approximately similar with respect to that of pure 5CB. Singh et al have reported that due to dispersion of BTNPs in NLC conductivity anisotropy increases [39]. Whereas for 5.0 wt% BTNPs composite,$\sigma_{i\parallel}$ decreases as compared to pure 5 CB. At 23.0 °C, the $\sigma_{i\parallel}$ are 9.40×10^{-7} S m^{-1} for pure 5CB and that of composites are 6.67×10^{-5} S m^{-1} (0.05 wt %), 9.91×10^{-7} S m^{-1} (0.5 wt %) and 1.78×10^{-7} S $m^{-1}$for 5.0 wt%. The solid lines in **Figure 1.11 (a)**show Arrhenius behaviour of the conductivity. The reason of conductivity enrichment is that, availability of additional space facilitates the motion of ions in the samples [31].One important result is that with increase of the doping concentration, $\sigma_{i\parallel}$decreases because higher concentration formsnanoscale ferroelectric NPs aggregates [83-86]. According to Shaydyuk*et al* [87], higher concentrations (4.5 wt %) of montmorillonite (MMT) nanoplatelets in 5CB show strong tendency of aggregation. Due to this in the case of higher concentrations (5.0 wt% BTNs), $\sigma_{i\parallel}$ is decreases in our case as well. I have create enhancement in the only longitudinal component of the $\sigma_{i\parallel}$ due to the facile motion of BTNPs in the longitudinal direction of the nematic director. The unchanged value of the$\sigma_{i\perp}$signifies that there is no significant movement of BTNPs along the transverse direction of the nematic director.

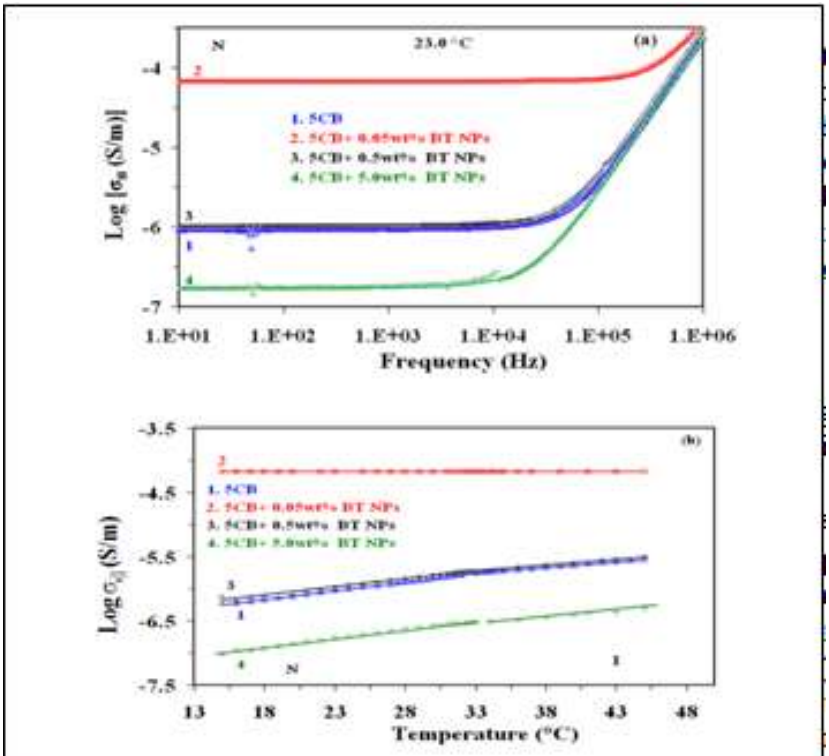

Figure 11: (a) Variation of conductivity along to the director ($\sigma_{\parallel}$) with frequency and (b) variation of the logarithm of ionic conductivity along to the director ($\sigma_{\parallel}$) with temperature for pure 5 CB and its nano composites. Curves 1, 2, 3 and 4 correspond to the pure 5CB, 5CB + 0.05 wt % BTNPs, 5CB + 0.5 wt % BTNPs and 5CB + 5.0 wt % BTNPs, respectively. The step like change seen in figure correspond to the T_{N} and the lines are just guides to the eye.

III. CONCLUSION

From the experimental observations and discussion, the followings can be concluded:

1. By escalating concentration of BTNPs in 5 CB it has been found that nematic-isotropic transition temperature decreases by 0.3 °C for 0.05 wt %, 1.3 °C for 0.5 wt % and 1.4 °C for 5.0 wt % of BTNPs.
2. Longitudinal component of the dielectric permittivity decreases appreciably though transverse component of the dielectric permittivity remains stable with rising concentration of BTNPs.Hence dielectric anisotropy too decreases by about 5 % for 0.05 wt %, 7 % for 0.5 wt % and 14 % for 5.0 wt % of BTNPs.
3. The relaxation frequencies of an observed relaxation mode corresponding to the flip-flop rotation of the molecules about their short axis initially decreases for 0.05 wt % but above this concentration they are increasing with the increasing concentration of BTNPs in 5CB.
4. The activation energies of an observed relaxation mode corresponding to the flip-flop rotation of the molecules about their short axis initially decreases for 0.05 wt % but above this concentration they are increasing with the increasing concentration of BTNPs in 5CB.

5. The longitudinal component of ionic conductivity has enlarged by about two orders of magnitude for 0.05 wt % BTNPs nanocomposites while on increasing concentration it decreases.
6. Optical band gap of 5CB (3.82 eV) has decreased to 3.80eV for 0.05 wt %, 3.81eV for 0.5 wt % and 3.81eV for 5.0 wt % of BTNPs.

7. Threshold voltage decreases by 2 % for 0.05 wt %, 17 % for 0.5 wt % and 8 % for 5.0 wt % due to dispersion of BTNPs in 5CB. Switching voltage, splay elastic unvarying have decreased whereas steepness of TVC curve has amplified.

REFERENCES

[1] P. P. Karat, N. V. Madhusudana. Mol. Cryst. Liq. Cryst. **36**, 51, 1976.
[2] D. Porter, J. R. Savage, I. Cohen. Phys. Rev. E. **85**, 041701, 2012.
[3] N. I. Lebovka , L. N. Lisetski , M. I. Nesterenko , V. D. Panikarskaya , N. A. Kasian , S. S. Minenko& M. S. Soskin. Liq. Cryst. **40**, 968, 2013.
[4] M. Kuzma, M. M. Labes. Mol. Cryst. Liq. Cryst. **100**, 103, 1983.
[5] U. Shivakumar, J. Mirzaei, X. Feng, A. Sharma, P. Moreira, T. Hegmann. Liq. Cryst. **38**, 1495, 2011.
[6] R. Verma, R. Dhar, R. Dabrowski, M. Tykarska, V. K. Wadhawan, M. C. Rath, S. K. Sarkar. J. Phys. D: Appl. Phys. **42,** 085503, 2009.
[7] R. Basu, G. S. Iannacchione. Appl. Phys. Lett. **93**, 183105, 2008.
[8] A. Schonhals, H. L. Zubora, R. S. Fricke, L. Frunza, R. Moldovan. Cryst. Res. Technol. **34**, 1309, 1999.
[9] S. Urban, B. Gestblom, R. Dabrowski. Phys. Chem. Chem. Phys. **1**, 4843, 1999.
[10] M. Kole, T. K. Dey. J. Appl. Phys. **113**, 084307, 2013.
[11] G. P. Sinha, F. M. Aliev. Phys. Rev. E. **58**, 1998, 2001.
[12] R. Basu, G. S. Iannacchione. J. Appl. Phys. **106**, 124312, 2009.
[13] J. Jadzyn, P. Kedziora. Mol. Cryst. Liq. Cryst. **145**, 17, 1987.
[14] P. G. Cummins, D. A. Dunmur, D. A. Laidler. Mol. Cryst. Liq. Cryst. **30**, 109, 1975.
[15] C. Dascalu, A.L. Alexe-Ionescu, G. Barbero. J. Electroanal. Chem. **767**, 63, 2016.
[16] F. Al-Hazmi, A. A. Al-Ghamdi, N. Al-Senany, F. Alnowaiser, F. Yakuphanoglu. J. Mol. Liq. **190**, 169, 2014.
[17] A. Bogi. S. Faetti. Liq. Cryst. **28**, 729, 2001.
[18] A.V. Zakharova, A. Maliniak. Eur. Phys. J. E. **4**, 435, 2001.
[19] S. Urban , H. G. Kreul, A. Wurflinger. Liq. Cryst. **12**, 921, 1992.
[20] A. Dawid, W. Gwizdala. Rev. Adv. Mater. Sci. **23**, 37, 2010.
[21] B. J. Frisken, P. P. Muhoray. Phy. Rev. A. **39**, 1513, 1989.
[22] J. F. Blach, S. Saitzek, C. Legrand, L. Dupont, J. F. Henninot, M. Warenghem. J Appl. Phys. **107**, 074102, 2010.
[23] S. P. Yadav, K. K. Pandey, A. K. Mishra, R. Manohar. Acta. Phys. Pol. A. **119**, 824, 2011.
[24] S. Oka, M. Kimura, T. Akahane. Appl. Phys. Lett. **80**, 1847, 2002.
[25] G. B. Hadjichristov, Y. G. Marinov, A. G. Petrov, L. Marino, N. Scaramuzz. J. Phys.: Conf. Ser. **682**, 012015, 2016.
[26] G. B. Hadjichristov, Y. G. Marinov, A. G. Petrov, E. Bruno, L. Marino, N. Scaramuzza. Mol. Cryst. Liq. Cryst. **610**, 135, 2015.
[27] D. Rajh, S. SHelestick, A. Mertelj, P. Umek, S. Irusta, A. Zak, I. Dolenik. Phys. Status. Solidi A. **210**, 2328, 2013.
[28] F. Z. Elouali, D. A. Tabet, U. Maschke. Mol. Cryst. Liq. Cryst. **502**, 77, 2009.
[29] I. Chashechnikova, L. Dolgov, T. Gavrilko, G. Puchkovska, Ye. Shaydyuk, N. Lebovka, V. Moraru, J. Baran, H. Ratajczak. J. Mol. Struct. **563**, 744, 2005.
[30] J. Baran, L. Dolgov, T. Gavrilko, L. Osinkina, G. Puchkovska, H. Ratajczak, Y. Shaydyuk, A. Hauser. Phils. Mag. **87**, 4273, 2007.
[31] A. S. Pandey, R. Dhar, S. Kumar, R. Dabrowski. Liq. Cryst. **38**, 115, 2011.
[32] T. Bezrodna, I. Chashechnikova, T. Gavrilko, G. Puchkovska, Y. Shaydyuk, A. Tolochko, J. Baran, M. Drozd. Liq. Cryst. **35**, 265, 2008.
[33] P. P. Korneychuk, O. G. Tereshchenko, Y. A. Reznikov, V. Yu. Reshetnyak, K. D. Singer. J. Opt. Soc. Am. B. **23**, 1007, 2006.

[34] M. V. Rasna, L. Cmok, D. R. Evans, A. Mwrtelj, S. Dhara. Liq. Cryst. **42**, 1059, 2015.
[35] V. G. Chigrinov. Liquid Crystal Devices: Physics and Applications. Bostan, MA: Artech House, 1999.
[36] R. Dhar. Liquid Crystals: Electrical, Optical and Thermodynamical Properties. D. Phil. Thesis submitted to the University of Allahabad, Allahabad, India, 1996.
[37] R. Dhar, R. S. Pandey, V. K. Agrawal. Indian. J. Pure Appl. Phys. **40**, 901, 2002.
[38] M. Kaczmarek, O. Buchnev, I. Nandhkumar. Appl. Phys. Lett. **92**, 103307, 2008.
[39] U. B. Singh, R. Dhar, R. Dabrowski, M. B. Pandey. Liq. Cryst. **41**, 953, 2014.
[40] F. Li, O. Buchnev, C. Cheon, A. Gluushchenko, V. Resshetnyak, Y. Reznikov, T. J. Sluckin, J. L. West. Phys. Rev. Lett. **97**, 147801, 2006.
[41] F. Li, J. West, A. Glushchenko, C. Cheon, Y. Reznikov. J. SID. **14**, 523, 2006.
[42] Y. Lin, R. Douali, F. Dubois, A. Segovia-Mera, A. Daoudi.Eur. Phys. J. E. **38**, 103, 2015.
[43] O. Kurochkin, H. Atkuri, O. Buchnev, A. Glushchenko, O. Grabar, R. Karapinar, V. Reshetnyak, J. West, Y. Reznikov. Condens. Matter. Phys. **13**, 33701, 2010.
[44] O. Kurochkin, O. Buchnev, A. Iijin, S. K. Park, S. B. Kown, O. Grabar, Y. Reznikov, A colloid of ferroelectric nanoparticles in a cholestric liquid crystal, J. Opt. A: Pure Appl. Opt. **11**, 024003, 2009.
[45] A. Lorenz, N. Zimmermann, S. Kumar, D. R. Evans, G. Cook, M. F. Martinez, H. S. Kitzerow. J. Phys. Chem. B. **117**, 937, 2013.
[46] M. V. Gorkunov, M. A. Osipov. Soft matter. **7**, 4348, 2011.
[47] L. M. Lopatina, J. V. Selinger. Phys. Rev. Lett. **102**, 197802, 2009.
[48] M. Gupta, I. Satpathy, A. Roy. R. Pratibha. J. Colloid. Interface. Sci. **352**, 292, 2010.
[49] M. V. Gorkunov, G. A. Shandryuk, A. M. Shatalova, I. Y. Kutergina, A. S. Merekalov, Y. Kudryavtsev, R. V. Talroze, M. A. Osipov. Soft Matter. **9**, 3578, 2013.
[50] K. K. Vardanyan, R. D. Walton, D. M. Bubb. Liq. Cryst. **38**, 1279, 2011.
[51] S. T. Wu. J. Appl. Phys. **69**, 2080, 1991.
[52] M. R. A. Bhuiyan, M. M. Alam, M. A. Momin, M. J. Uddin, M. Islam. Int. J. Matter. Mech. Engg. **1**, 21, 2012.
[53] J. Tauc. Amorphous and liquid semiconductor. Plenum. New York, 1974.
[54] J. Tauc. A. Menth. Non. Cryst. Solids. **8**, 569, 1972.
[55] O. Harizanov, A. Harizanova, T. Ivanova. Mater. Sci. Eng. B. **106**, 191, 2004.
[56] R. Ashiri, A. Nemati, M. S. Ghamsari, H. Aadelkhani. J. Non. Cryst. Solids. **355**, 2480, 2009.
[57] H. X. Zhang, C. H. Kam, Y. Zhou, X. Q. Han, Y. L. Lam, Y. C. Chan, K. Pita. Mater. Chem. Phys. **63**, 174, 2000.
[58] S. H. Wemple. Phys. Rev. B. **2**, 2679, 1970.
[59] T. D. Ibragimov, A.R. Imamaliyev, G.M. Bayramov. Optik. **127**, 2278, 2016.
[60] C. Cirtoaje, E. Petrescu, V. Stoian. Physica E. **67**, 23, 2015.
[61] Y. Reznikov, O. Buchnev, O. Tereshchenkov, V. Reshetnyak, A. Glushchenko, J. West. Appl. Phys. Lett. **82**, 1917, 2003.
[62] U. B. Singh, M. B. Pandey, R. Dhar, R. Verma, S. Kumar. Liq. Cryst. 2016 http://dx.doi.org/10.1080/02678292.2016.1159344
[63] R. Dhar, A. S. Pandey, M. B. Pandey, S. Kumar, R. Dabrowski. Appl. Phys. Express. **1**, 12501, 2008.
[64] K. K. Vardanyan, D. M. Sita, R. D. Walton, W. M. Saideld, K. M. Jones. RSC Adv. **3**, 259, 2013.
[65] P. G. de Gennes, J. Prost. The Physics of Liquid Crystals. 2nd ed., Clarendon Press, Oxford, 1993.
[66] F. Haraguchi, K. I. Inoue, N. Toshima, S. Kobayashi, K. Takatoh. Jpn. J. Appl. Phys. **46**, L796, 2007.
[67] W. Maier, G. Meier. Z. Naturforsch. **16**, 262, 1961.
[68] J. G. Kirkwood. J. Chem. Phys. **7**, 911, 1939.
[69] K. K. Vardanyan, E. D. Palaazzo, R. D. Walton. Liq. Cryst. **38**, 709, 2011.
[70] R. Nozaki, T. K. Bose, S. Yagihara, Phys. Rev. A. **46**, 7733, 1992.
[71] H. Kresse, H. Stettin, F. Gouda, G. Anderson. Phys. Status Solidi A. **111**, K265, 1989.
[72] S. Mohyeddine, M. B. Pandey, D. Revannasiddaiah. Phase Transitions. **82**, 11, 2009.
[73] K. S. Cole, R. H. Cole, R. H. J. Chem. Phys. **9**, 341, 1941.
[74] M. B. Pandey, R. Dhar, V. K. Agrawal, R. Dabrowski. Mol. Cryst. Liq. Cryst. **414**, 63, 2004.
[75] M. B. Pandey, R. Dabrowski, R. Dhar. Ferroelectrics. **395**, 99, 2010.
[76] O. Koysal, M. Okutan, M. Durmuş, F. Yakuphanoglu, S.E. San, V. Ahse. Synt. Met.**156**, 58, 2006.
[77] C. J. F. Bottcher, P. Bordewijk. Theory of Electric Polarization, Vol II. Elsevier, Amsterdam, 1978.
[78] N. Yadav, R. Dabrowski, R. Dhar. Liq. Cryst. **41**, 1803, 2014.
[79] N. E. Hill, W. E. Hill, A. H. Price, M. Davis. Dielectric properties and molecular behaviour. London: Van Nostrand Reinhold, 1991.
[80] M. B. Pandey, R. Dhar, V. K. Agrawal, R. P. Khare, R. Dabrowski. Phase Transitions. **76**, 945, 2003.

[81] B. Kamaliya, M. V. Kumar, C. V. Yelamaggad, S. K. Prasad. Appl. Phys. Lett. **106**, 083110, 2015.
[82] S. L. Srivastava, R. Dhar. Radiat. Phys. Chem. **47**, 287, 1996.
[83] R. Basu, A. Garvey. Appl. Phys. Lett. **105**, 151905, 2014.
[84] S. P. Meeker, M. C. K. Poon, J. Crain, E. M. Terentjev. Phys. Rev. E. **61**, 6083, 2000.
[85] V. J. Anderson, E. M. Terentjev, S. P. Meeker, J. Crain, W. C. K. Poon, Eur. Phys. J. E. **4**, 11, 2001.
[86] S. P. Yadav, R. Manohar, S. Singh. Liq. Cryst. **42**, 1095, 2015.
[87] Y. Shaydyuk, G. Puchkovska, A. Goncharuk, N. Lebovka. Liq. Cryst. **38**, 155, 2011.
[88] M. R. Herrington, O. Buchnev, M. Kaczmarek, I. Nandhkumar. Mol. Cryst. Liq. Cryst. **527**, 72, 2010.
[89] A. Glushchenko, C. Cheon, J. West, F. Li, E. Buyuktanir, Y. Reznikov, A. Buchnev. Mol. Cryst. Liq. Cryst. **453**, 227, 2006.
[90] S. N. Paul, R. Dhar, R. Verma, S. Sharma, R. Dabrowski. Mol. Cryst. Liq. Cryst. **545**, 105, 2011.

